

# Letters

## On the Equilibrium Points in Three-Phase PLL Based on the $d$ -axis Voltage Normalization

Chao Wu <sup>✉</sup>, *Member, IEEE*, Xiaoling Xiong <sup>✉</sup>, *Member, IEEE*, Mads Graungaard Taul <sup>✉</sup>, *Member, IEEE*, and Frede Blaabjerg <sup>✉</sup>, *Fellow, IEEE*

**Abstract**—Voltage normalization is usually adopted for a phase-locked loop (PLL) to keep a constant bandwidth unaffected from the voltage magnitude at the point of synchronization. Two conventional PLL normalization methods are analyzed from a large-signal perspective in this letter. However, different from the voltage magnitude normalization method, an unexpected stable equilibrium point emerges in the three-phase PLL based on the  $d$ -axis voltage normalization, the mechanism of which is revealed by the phase-plane analysis. Due to the unexpected equilibrium point, the  $d$ -axis voltage normalization will lose the phase tracking ability when the initial phase difference or phase jump exceeds  $\pi/2$ . Thus, it is suggested to use the magnitude normalization instead of the  $d$ -axis voltage normalization to avoid this kind of malfunction. Finally, the experimental results validate the theoretical analysis.

**Index Terms**—Equilibrium point, large-signal analysis, phase-locked loop (PLL), voltage normalization.

### I. INTRODUCTION

OVER the past decades, converter-based renewable power generation has been widely integrated into the power grids [1]. The basic requirement of these installed renewable power generations is to achieve precise power control. The accurate and stable power control of the converter is highly dependent on the synchronization block, which is applied for acquiring the grid voltage angle [2], [3]. Among all synchronization blocks, the phase-locked loop (PLL) is the most commonly used synchronization method for the power converter. Thus, it is of significant importance to study the performance of PLL.

There are a lot of research works about the PLL studies [4]–[15]. The main objective of the PLL is to track the grid voltage angle quickly and accurately [4]–[6]. From this perspective, the bandwidth of PLL should be designed high enough to maintain good dynamic performance of phase tracking. However, under weak-grid conditions, a high bandwidth will cause instability since the PLL will introduce a negative resistance behavior to the current control [7]. Thus, between

the fast phase tracking and the stability requirement, the bandwidth of the PLL should be designed carefully to make a compromise between these two performances.

In order to have a unified bandwidth design method for PLL under different voltage levels, voltage normalization is usually applied to eliminate the effect of voltage magnitude on the PLL dynamics. To this end, an amplitude normalization scheme is often included in the PLL structure to keep the dynamic and stability characteristics of the PLL decoupled from the variations of voltage. Straightforwardly, the voltage normalization can be achieved by simply dividing voltage magnitude (DVM) in the stationary frame [8]. Furthermore, directly dividing  $d$ -axis voltage (DDV) can also be used for the voltage normalization [6], [9], [14]. In [10]–[12], an alternative approach for amplitude normalization is using the inverse tangent operation, which reduces the nonlinearity of the PLL control loop at the cost of a higher computational effort. All these methods can achieve voltage normalization to keep a constant bandwidth. However, only the small-signal response is analyzed in the prior-art research without considering the large-signal performance. In [13], an adaptive PLL structure is proposed for fast and smooth tracking of phase-angle jumps. Furthermore, the magnitude is also used for the voltage normalization in the single-phase enhanced PLL [14]. Even though another stable equilibrium point is shown by the phase portraits, the intrinsic reason is not revealed and a comprehensive comparison between the different normalization methods is absent. Namely, what is the dynamic response difference between the different normalized PLLs when there is an initial phase-angle difference or a sudden phase jump? This question will be answered in this letter.

In this letter, the nonlinear mathematical models of the two widely used normalized PLLs are built for a comprehensive comparison from a large-signal perspective. Surprisingly, it is discovered that the widely used  $d$ -axis voltage normalization method will have an unexpected equilibrium point, which may cause a wrong tracking phase angle. Thus, using the voltage magnitude division instead of the  $d$ -axis voltage division for the voltage normalization to avoid the unexpected wrong equilibrium point is highly suggested. Finally, the experimental results are conducted to verify the theoretical analysis.

### II. MATHEMATICAL MODELS OF NORMALIZED PLLS

The topology of the grid-connected converter is illustrated in Fig. 1.  $U_{gabc}$  represents the three-phase grid voltage,  $I_{gabc}$  represents the three-phase current injected into the grid,  $L_{cf}$  is the converter filter that is applied for suppressing current harmonics, and  $U_{dc}$  is the dc-link voltage. It should be noted that, in practice, a grid impedance will add another destabilizing term, which further challenges the system stability [3]. Thus, the grid impedance is not considered since the main focus of this work is to study the phase tracking ability of the normalized

Manuscript received March 3, 2021; revised April 6, 2021; accepted April 19, 2021. Date of publication April 22, 2021; date of current version July 30, 2021. This work was supported in part by THE VELUX FOUNDATIONS under the VILLUM Investigator Grant REPEPS under Award No. 00016591 and in part by the National Natural Science Foundation of China under Grant 51707065. (Corresponding author: Xiaoling Xiong.)

Chao Wu and Frede Blaabjerg are with the Department of Energy Technology, Aalborg University, 9220 Aalborg, Denmark (e-mail: cwu@et.aau.dk; fbl@et.aau.dk).

Xiaoling Xiong is with the State Key Laboratory of Alternate Electrical Power System with Renewable Energy Sources, North China Electric Power University, Beijing 102206, China (e-mail: xiongxl1102@ncepu.edu.cn).

Mads Graungaard Taul is with the Energinet, 7000 Fredericia, Denmark (e-mail: mkg@et.aau.dk).

Color versions of one or more figures in this article are available at <https://doi.org/10.1109/TPEL.2021.3074986>.

Digital Object Identifier 10.1109/TPEL.2021.3074986

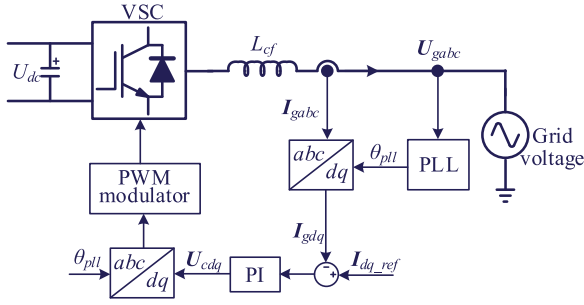


Fig. 1. General topology and control scheme of a three-phase grid-connected converter with the current vector control.

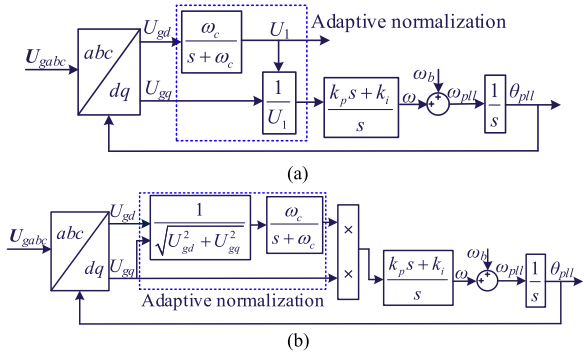


Fig. 2. Structures of two different normalized PLLs. (a) DDV-PLL. (b) DVM-PLL.

PLLs. The block PLL is applied to estimate the angle of grid voltage. In order to maintain a constant bandwidth and damping ratio, voltage normalization methods are always introduced into the PLL block. In this letter, the two commonly used normalized PLL structures are discussed and compared from a large-signal perspective.

The structures of two typical normalized PLLs are shown in Fig. 2. In order to do simplification, the DDV-PLL and DVM-PLL represent the normalization based on DDV and DVM, respectively. The input is the three-phase grid voltage  $U_{gabc}$ , and the output is the estimated angle of grid voltage, which is denoted as  $\theta_{pll}$  to distinguish it from the grid voltage angle  $\theta_g$ . In the steady state,  $\theta_{pll} = \theta_g$ . However, during the transient period, such as the initial startup or phase jump of grid voltage,  $\theta_{pll} \neq \theta_g$ , and the PLL angle will try to track the grid voltage angle quickly to eliminate the angle error.  $\omega_b$  is a constant frequency feedforward term, which is  $100\pi$  rad/s in this letter,  $\omega_{pll}$  is the PLL angular frequency, and  $f_{pll} = \omega_{pll}/(2\pi)$  is the PLL frequency.  $k_p$  and  $k_i$  are the proportional and integral parameters of the proportional and integral (PI) controller applied in the normalized PLLs.

It should be noted that the low-pass filter is only employed for eliminating the noise caused by the division part. Thus, the cutoff frequency  $\omega_c$  can be set high enough without affecting the PLL dynamics. In this letter, the bandwidth of PLL is chosen at 30 Hz, and the cutoff frequency of the LPF is set at 300 Hz. To this end, the effect of the LPF can be ignored when analyzing the dynamic performance of PLL.

Without considering the LPF, the  $dq$  axes' voltages in Fig. 2 can be expressed as

$$\begin{aligned} U_{gd} &= U_g \cos(\theta_g - \theta_{pll}) = U_g \cos \delta \\ U_{gq} &= U_g \sin(\theta_g - \theta_{pll}) = -U_g \sin \delta \end{aligned} \quad (1)$$

where  $U_g$  is the magnitude of grid voltage, and the angle difference between the PLL angle and grid voltage angle is defined as  $\delta = \theta_{pll} - \theta_g$ .

Thus, the simplified large-signal model of the two normalized PLL methods can be illustrated in Fig. 3, where the  $q$ -axis voltage can be

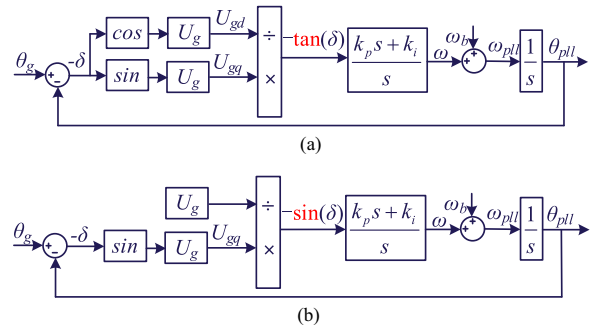


Fig. 3. Simplified large-signal model of the two normalized PLLs in Fig. 2. (a) DDV-PLL. (b) DVM-PLL.

According to the large-signal model in Fig. 3, it can be seen that the dynamics of the normalized PLL is a second-order nonlinear system, and  $\delta$  and  $\omega$  are chosen as the state variables. Consequently, the state-space model of the DDV-PLL in Fig. 3(a) can be expressed as

$$\begin{cases} \dot{\delta} = (\omega + \omega_b - \omega_g) \\ \dot{\omega} = \frac{-\delta k_p}{(\cos \delta)^2} - k_i \tan \delta. \end{cases} \quad (2)$$

The state-space model of the DVM-PLL in Fig. 3(b) can be derived as

$$\begin{cases} \dot{\delta} = (\omega + \omega_b - \omega_g) \\ \dot{\omega} = -\delta k_p \cos \delta - k_i \sin \delta. \end{cases} \quad (3)$$

As can be seen from (2) and (3), the second-order differential equations are different with different normalization schemes. In order to make a more intuitive comparison between the two normalization methods, the large-signal analysis based on the phase-plane analysis is conducted Section III.

### III. LARGE-SIGNAL ANALYSIS OF NORMALIZED PLLS

#### A. Phase-Plane Analysis

In order to analyze the large-signal stability performance, the phase-plane analysis method is used. It is well known that the initial angle difference between the grid voltage angle and the PLL angle can be any angle in the range  $[-\pi/2, 3\pi/2]$  or  $[-\pi, \pi]$ . A phase jump can be seen as the same disturbance type as an initial angle difference. Thus, only the initial angle difference is mentioned in the following analysis. To guarantee the phase tracking ability of the normalized PLL, the angle  $\delta$  should come back to zero under any kind of initial angle difference. In this way, to check the angle tracking ability of the normalized PLLs, the phase portraits of the two different normalization methods with different initial angle differences are plotted in Fig. 4. It should be noted that  $\delta$  is chosen as the  $y$ -axis in Fig. 4 but not the angular frequency  $\omega$ . Thus, the phase portrait in Fig. 4 is also correct when considering the grid frequency deviations.

Fig. 4(a) shows the phase portrait of DDV-PLL with different initial states. Four different initial angle differences  $\delta_0$  are checked based on the differential equations in (2). From Fig. 4(a), when the initial angle differences are between  $[-\pi/2, \pi/2]$ , such as  $-\pi/4$  and  $\pi/4$ , the angle difference  $\delta$  can converge to 0 in the steady state, which means that the PLL works normally under these conditions. However, when the initial angle differences are between  $[\pi/2, 3\pi/2]$ , such as  $3\pi/4$  and  $5\pi/4$ , the angle difference  $\delta$  will converge to  $\pi$  in the steady state, which means there is a large steady-state error between the grid voltage angle and the PLL angle. Under these conditions, the DDV-PLL will lose the phase tracking ability. It should be kept in mind that the objective of PLL is to track the angle without the steady-state error. What we anticipate for PLL is that the output angle can always be equal to the grid voltage

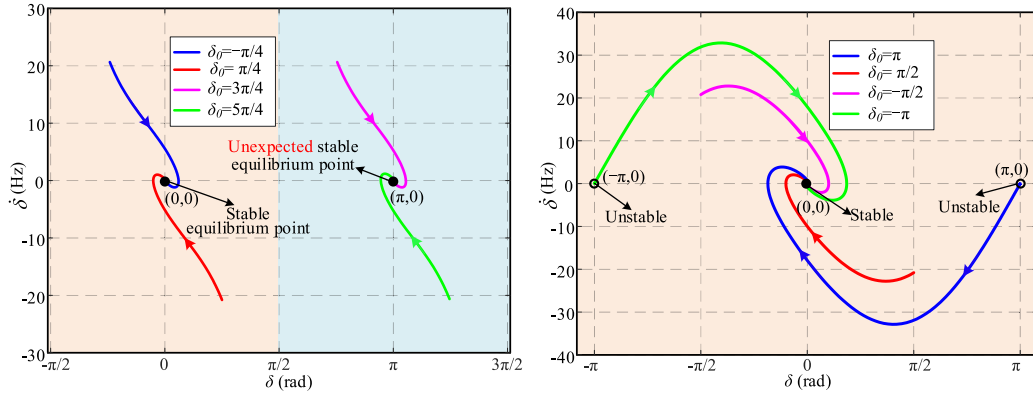


Fig. 4. Phase portraits of two normalized PLLs with different initial angle differences. (a) Phase portrait of DDV-PLL. (b) Phase portrait of DVM-PLL.

see, the steady-state angle error will be  $180^\circ$  when the phase jumps larger than  $90^\circ$ , and this is not acceptable in the real case. Thus, this stable equilibrium point is called “unexpected.” The steady-state angle error  $\pi$  could cause the power flow direction of the converter reversed, which can cause instability or damages to the dc-link. This should be avoided in real applications.

Fig. 4(b) shows the phase portrait of DVM-PLL with different initial angle differences. Four different initial angle differences  $\delta_0$  are checked based on the differential equations in (3). The maximum initial angle differences are  $\pi$  and  $-\pi$ . As can be seen from Fig. 4(b), the angle  $\delta$  can always come back to 0 no matter which initial angle is, which proves that this kind of normalized PLL can always track the grid voltage angle under any kind of phase jumps. Thus, the DVM-PLL has a more robust response to the variations of the grid voltage phase jumps, which is preferably recommended for real applications.

### B. Mechanism Analysis

From the above, it is desirable to answer the following questions: Why is there a significant difference between the two normalization methods, and how can this phenomenon be explained? The answers to those will be detailed in the following.

As can be seen from Fig. 4, the main difference between these two normalized PLLs is the stable equilibrium point difference. For the DVM-PLL, there is only one stable equilibrium point during the  $2\pi$  range. However, for the DDV-PLL, there are two equilibrium points during  $2\pi$  range, which is the main reason that causes the malfunction of PLL during large initial angle difference.

To identify which operating point is stable or unstable, the simplest way is to check the slope of the equilibrium points. Based on (2) and (3), setting the differential terms in (2) and (3) to be zero, the equilibrium points can be obtained. From (2), the equilibrium point is dependent on the tangent function, while the equilibrium point is dependent on the sine function in (3). Thus, the waveforms of sine and tangent function in the  $2\pi$  range are plotted in Fig. 5. It can be seen the two normalized PLLs both have two equilibrium points 0 and  $\pi$ .

However, for the sine function in Fig. 5(a), the slope of the equilibrium point at  $\pi$  is negative, which means this equilibrium point is unstable. From Fig. 5(b), it is easy to find that both the two equilibrium points are stable for the tangent function. Thus, when the phase angle jumps more than  $\pi/2$  from the zero point, the angle difference will converge to another equilibrium point  $\pi$ . Even though the PLL can operate stably at this equilibrium point, the angle acquired from the PLL is not the same as the grid voltage angle, which has a steady-state error  $\pi$ . To this end, the phase detector changing from sine function to

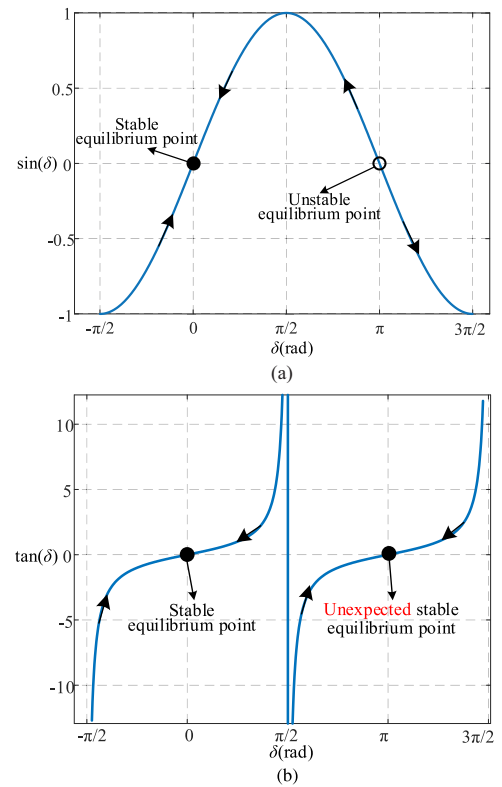


Fig. 5. Waveforms of sine and tangent function in  $2\pi$  range. (a) Waveforms of the sine function. (b) Waveforms of the tangent function.

tangent function is the fundamental reason that causes this unexpected stable equilibrium point in DDV-PLL.

## IV. EXPERIMENTAL VALIDATION

To verify the theoretical analysis, the experiments for the two normalized PLLs are carried out in the lab shown in Fig. 6. A 45-kVA Chroma 61845 grid simulator is used for generating the three-phase grid voltage, and the DS2400 A/D board is used to sample the grid voltage, which is then sent to the dSpace DS1007, where the control strategy is implemented. The DS2102 D/A board is used to output the waveforms. The peak value of the phase voltage is 325 V and the grid frequency is 50 Hz. The cutoff frequency  $\omega_c$  is chosen as 1885 rad/s,  $k_p$  is 130, and  $k_i$  is 7750, which are large due to the normalization.

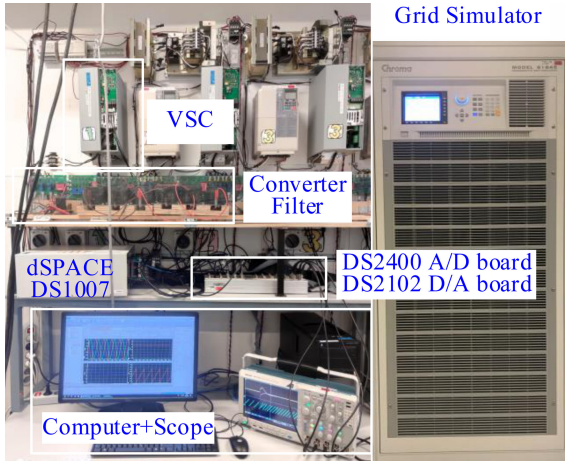


Fig. 6. Laboratory setup for the experimental verification.

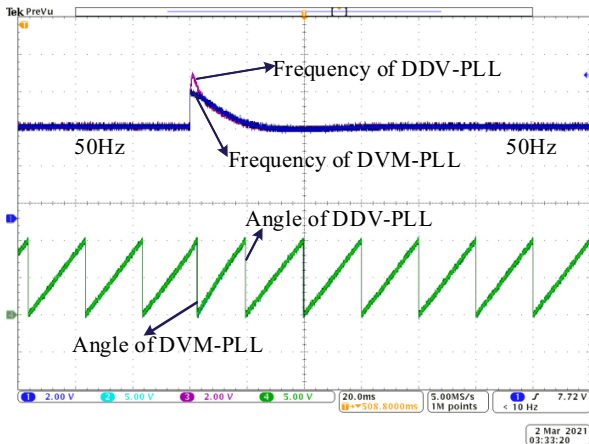


Fig. 7. Experimental results of normalized PLLs during sudden phase jump  $\pi/3$ .

Fig. 7 shows the experimental results when the phase jump is  $\pi/3$ . When the phase jump occurs, the frequency will have a sudden jump. However, the frequency deviation of the DDV-PLL is higher than the DVM-PLL because the tangent function is larger than the sine function when the angle is large. However, both the two normalized PLLs can track the grid voltage angle since the angle  $\delta$  can come back to zero in the steady state and the two PLL angles are completely coincident. Since the angle of the grid voltage and the normalized PLLs are both sawtooth waveforms changing from 0 to  $2\pi$ , the phase error is not ideally 0 but jumping from 0 to  $2\pi$  due to the digital controller. Thus, the phase error is not shown in the experimental results but directly showing the frequency and angle, which are more clear to show the dynamic process during the phase jumps.

Fig. 8. shows the experimental results when the phase jump is  $3\pi/4$ . Due to the sudden phase change exceeds  $\pi/2$ , the  $d$ -axis voltage will be negative and will cause the angle  $\delta$  to converge to  $-\pi$ . In this way, the DDV-PLL will lose the phase tracking ability but the DVM-PLL can still be capable of tracking the phase even when the phase jump is so large. Thus, there will be a constant angle error  $\pi$  between the angle of DDV-PLL and DVM-PLL. These experimental results agree well with the theoretical analysis with the phase portraits, as depicted in Fig. 4, which further confirms the correctness of the theoretical findings.

In order to validate the unexpected equilibrium point that exists in other improved PLL structures, the experimental results of DDV-PLL

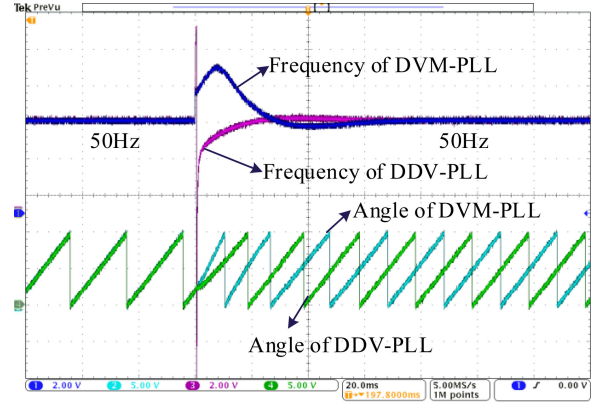


Fig. 8. Experimental results of normalized PLLs during sudden phase jump  $3\pi/4$ .

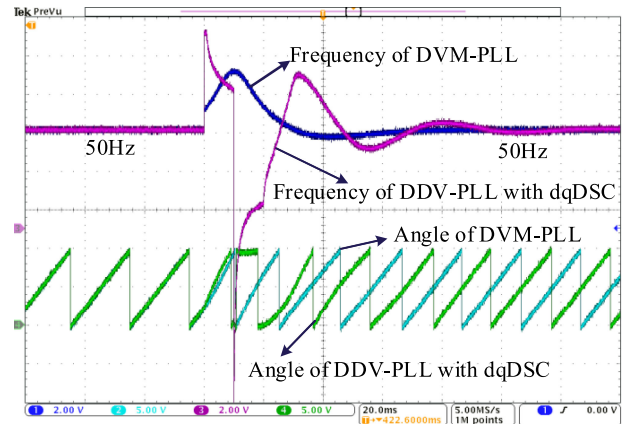


Fig. 9. Experimental results of normalized PLLs during sudden phase jump  $5\pi/6$ .

with  $dq$ -frame delayed signal cancellation ( $dqDSC$ ) under phase jump  $5\pi/6$  are shown in Fig. 9. The  $dqDSC$  block is added in the PLL for eliminating the negative effect of the dc offset and odd harmonics [15]. Since the  $dqDSC$ -PLL is still directly using the  $d$ -axis voltage for normalization, it will cause a steady phase error during a large phase jump. Thus, the conclusion obtained from the simple DDV-PLL structure, as shown in Fig. 2(a), is applicable for any other kinds of improved PLL structures, which are using the  $d$ -axis voltage for normalization without any correction to the output angle.

## V. CONCLUSION

In this letter, the detailed nonlinear mathematical models of two widely used normalized PLLs are built for performance comparison from a large-signal perspective. It is revealed that there is an unexpected stable equilibrium point in the DDV-PLL, resulting in tracking problems when the initial angle difference or phase jump exceeds  $\pi/2$ . The root cause is that DDV causes the phase detector to be a tangent function instead of a sinusoid function. Finally, the experimental results verified these important findings, and it is highly recommended to use the voltage magnitude instead of the  $d$ -axis voltage for normalization in the PLL. It should be noted that the conclusion can also be extended to single-phase PLLs. When the phase detector is mathematically equivalent to the tangent function, one should always be careful and recognize that an unexpected stable equilibrium point  $(\pi, 0)$  exists.

## REFERENCES

- [1] J. Rocabert, A. Luna, F. Blaabjerg, and P. Rodriguez, "Control of power converters in ac microgrids," *IEEE Trans. Power Electron.*, vol. 27, no. 11, pp. 4734–4749, Nov. 2012.
- [2] F. Blaabjerg, R. Teodorescu, M. Liserre, and A. V. Timbus, "Overview of control and grid synchronization for distributed power generation systems," *IEEE Trans. Ind. Electron.*, vol. 53, no. 5, pp. 1398–1409, Oct. 2006.
- [3] M. G. Taul, X. Wang, P. Davari, and F. Blaabjerg, "An overview of assessment methods for synchronization stability of grid-connected converters under severe symmetrical grid faults," *IEEE Trans. Power Electron.*, vol. 34, no. 10, pp. 9655–9670, Oct. 2019.
- [4] A. J. Viterbi, "Acquisition and tracking behavior of phase-locked loops," in *Proc. Symp. Active Netw. Feedback Syst.*, Apr. 1960, pp. 583–619.
- [5] V. Kaura and V. Blasko, "Operation of a phase locked loop system under distorted utility conditions," *IEEE Trans. Ind. Appl.*, vol. 33, no. 1, pp. 58–63, Jan./Feb. 1997.
- [6] S. Golestan, J. M. Guerrero, and J. C. Vasquez, "Three-phase PLLs: A review of recent advances," *IEEE Trans. Power Electron.*, vol. 32, no. 3, pp. 1894–1907, Mar. 2017.
- [7] B. Wen, D. Boroyevich, R. Burgos, P. Mattavelli, and Z. Shen, "Analysis of D-Q small-signal impedance of grid-tied inverters," *IEEE Trans. Power Electron.*, vol. 31, no. 1, pp. 675–687, Jan. 2016.
- [8] M. G. Taul, X. Wang, P. Davari, and F. Blaabjerg, "Robust fault ride through of converter-based generation during severe faults with phase jumps," *IEEE Trans. Ind. Appl.*, vol. 56, no. 1, pp. 570–583, Jan./Feb. 2020.
- [9] S. Golestan, J. M. Guerrero, J. C. Vasquez, A. M. Abusorrah, and Y. Al-Turki, "A study on three-phase PLLs," *IEEE Trans. Power Electron.*, vol. 34, no. 1, pp. 213–224, Jan. 2019.
- [10] S. Golestan, F. D. Freijedo, A. Vidal, J. M. Guerrero, and J. Doval-Gandoy, "A quasi-type-1 phase-locked loop structure," *IEEE Trans. Power Electron.*, vol. 29, no. 12, pp. 6264–6270, Dec. 2014.
- [11] I. Serban and C. Marinescu, "Control strategy of three-phase battery energy storage systems for frequency support in microgrids and with uninterrupted supply of local loads," *IEEE Trans. Power Electron.*, vol. 29, no. 9, pp. 5010–5020, Sep. 2014.
- [12] J.-W. Choi, Y.-K. Kim, and H.-G. Kim, "Digital PLL control for single phase photovoltaic system," *IEE Proc. - Electr. Power Appl.*, vol. 153, no. 1, pp. 40–46, Jan. 2006.
- [13] M. Karimi Ghartemani, S. A. Khajehoddin, P. K. Jain, and A. Bakhshai, "Problems of startup and phase jumps in PLL systems," *IEEE Trans. Power Electron.*, vol. 27, no. 4, pp. 1830–1838, Apr. 2012.
- [14] M. Karimi-Ghartemani, "Linear and pseudolinear enhanced phase-locked loop (EPLL) structures," *IEEE Trans. Ind. Electron.*, vol. 61, no. 3, pp. 1464–1474, Mar. 2014.
- [15] S. Golestan, J. M. Guerrero, and G. B. Gharehpetian, "Five approaches to deal with problem of DC offset in phase-locked loop algorithms: Design considerations and performance evaluations," *IEEE Trans. Power Electron.*, vol. 31, no. 1, pp. 648–661, Jan. 2016.